© JAN 2026 | IRE Journals | Volume 9 Issue 7 | ISSN: 2456-8880
DOI: https://doi.org/10.64388/IREV9I7-1713397

Liquid Loading Prediction in Deviated Wells: An Explorative Analysis of the Possibility of Complex Interplay Between the Entrained Droplet Model and Continuous Film Model

MEPAIYEDA ESTHER BUKOLA[1], OYEGBILE MARVELLOUS[2], SALIU FEMI[3], ISEHUNWA SUNDAY[4]

[1, 2]*Department of Petroleum and Gas Engineering, University of Lagos, Lagos State, Nigeria*
3Pillar Oil Limited, Nigeria
[4]*University of Ibadan, Oyo State, Nigeria*

Abstract- ***Liquid loading in gas wells remains a critical challenge, particularly in deviated and horizontal wells where multiphase flow dynamics become increasingly complex. Traditional models such as the Entrained Droplet Model (EDM) and the Continuous Film Model (CFM) have independently provided frameworks for understanding flow regimes and predicting critical velocities. However, recent investigations suggest that the interaction between these two fundamental models may not be entirely isolated, especially under varying well inclinations and flow conditions. This study aims to explore the potential complex interplay between the two models in deviated wells, proposing that a hybrid understanding could bridge the prediction accuracy gap for critical velocities. By leveraging empirical data and machine learning regression techniques, the analysis evaluates the transitions between droplet-dominated flow and film-dominated flow, offering insights into optimized flow predictions for gas wells unloading. Results show that by combining EDM and CFM, a more accurate prediction of the loading onset was achieved. Although the two models align in near-vertical wells, their predictions diverge at 30 - 60 degrees medium inclinations, where increased film thickness and reduced gravity raised the required critical velocity. In these cases, CFM tends to overpredict loading while EDM underpredicts it, indicating that neither model alone fully captures the onset of instability. By combining both criteria or applying an ML-assisted hybrid, prediction accuracy improves markedly, achieving R^2 values of ~0.93 for load classification and ~0.96 for critical-velocity regression. This confirms that an integrated EDM–CFM approach more reliably represents liquid-loading behaviour in deviated wells and enhances deliquification decision-making.***

Key words: Continuous film model, Critical gas velocity, Entrained droplet model, Liquid loading,

I. INTRODUCTION

In gas wells, liquid loading denotes the accumulation of produced liquids in the tubing when the gas can no longer lift them, which occurs once the gas velocity falls below a critical value (Ikpeka et al., 2018). The gas phase then forms a central core while liquid collects as an annulus or slugs. As reservoir pressure declines late in life, the reduced gas rate causes liquids to build up and eventually create backpressure that halts flow (Abhulimen et al., 2022). Cruz and Wasan (2013) emphasize that liquid loading is among the most significant production problems in gas wells, with telltale signs including surface slugging, erratic production rates, and rising wellhead pressure, ultimately saturating the formation near the wellbore. Accurately predicting the onset of liquid loading is thus crucial to avoid well shut-in and to design deliquification measures.

Deviated or inclined wells complicate liquid-loading behavior because gravity causes liquid to pool along the lower side of the casing. He et al. (2024) notes “great differences” in liquid-loading dynamics between vertical and horizontal wells. Even a modest inclination such as at 15° leads to asymmetric annular flow, as shown by experiments that observed a heavy liquid film on the down-side of the pipe and earlier loading thresholds than in a purely vertical case “An Experimental Study of Liquid Loading of Vertical and Deviated Gas Wells”, 2013. In practice, this means conventional vertical-well correlations can

underpredict holdup in deviated wells. A reliable model must therefore account for the well's angle and the possibility of stratified flow.

Mechanistically, liquid removal has historically been described by two classical models. Turner et al. (1969) proposed both a Continuous Film Model (CFM) and an Entrained Droplet Model (EDM). In the CFM, it is assumed that liquid inevitably forms a thin film on the tubing walls, and that the gas must drag this annular film upward to unload the well. Mathematically, the critical gas velocity is derived from a momentum balance on the film, taking into account gas shear and film weight. In the EDM, by contrast, liquid is presumed to exist as discrete droplets entrained in the gas core. Loading is predicted by considering the largest droplet as a freely falling particle: the critical condition is when gas drag just balances the gravitational settling of the droplet. Each approach yields an expression for the minimum continuous flow rate needed to remove liquid. Turner's original droplet model gives a critical velocity proportional to:

$$V_c = \left(\frac{(\sigma(\rho_L-\rho_G))^{0.25}}{\rho_G^{0.5}}\right) \quad (1)$$

where σ is surface tension and ρ are densities. Subsequent studies have noted that neither model is universally superior. For example, Luo (2013) concluded that the CFM often better matches field data and likely dominates the accumulation mechanism, whereas the EDM is simpler to apply and may suffice when liquids remain finely dispersed. Experimental and numerical results suggest a complex transition: at higher gas velocities, entrained droplets can eventually coalesce into a continuous film (He et al., 2024). In practice the droplet model "has a wide range of advantages in computation" but can fail to predict loading in some inclined wells, whereas the film model, though physically representative, may underestimate critical velocity in low-liquid conditions. Despite the extensive development of each model, few prior works have explicitly blended them. Most comparative studies treat EDM and CFM separately (or choose one a priori). Luo (2013) and others have reviewed them but stopped short of combining their effects, and no standard "hybrid" mechanistic model exists for liquid loading. Instead, researchers have resorted to empirical adjustments or data-driven correlations. Recent efforts by Khamehchi et al. and others use machine learning on large datasets to predict critical velocity without direct mechanistic linkage. This highlights a gap: the possible synergy between the two removal mechanisms has not been systematically explored. The present work therefore investigates a conceptual hybrid model, examining whether a combined EDM–CFM framework can improve prediction of loading onset in deviated wells beyond the classical models.

II. RESEARCH ELABORATIONS

Various researchers have studied prediction of onset of liquid loading in gas wells. These studies are either based on developing novel models or modification of existing models to improve prediction of the onset of liquid loading. Liquid loading is commonly explained by two mechanisms of liquid transportation in gas wells: the liquid droplet reversal and liquid film reversal. All the developed models rely on one or all of these mechanisms of liquid transportation to predict onset of liquid loading.

The liquid-droplet entrainment model developed by Turner et al. (1969) is a most renowned method for predicting gas well liquid loading onset. The model postulates that due to droplet fall back in gas core, liquid loading occurs. Freely falling droplet in a gas column is under action of two forces; the Drag force due to gas (Fd) pulling upward and a gravitational force due to droplet weight (Fw) pulling in downward direction. The droplet moves upward if Fd > Fw and downward if Fd < Fw. When both forces balance each other, a terminal velocity is achieved. Terminal velocity is a function of size, shape and density of particle being suspended and viscosity and density of suspending fluid (Coleman, et al. 1991).

They compared Eqn. (1) with field data and found it matching 77 out of 90 tested wells. Turner et al concluded that an upward adjustment of 20% must be made in order to enhance matchability of the well data. To calculate the critical velocity using field units, the coefficient of the model in Eqn. (1) is replaced by 1.92 and all other inputs in field units. Coleman et al. (1991) applied the original Turner model to their well data and they achieved a good match, whereas Turner's corrected model did not fit their well data. Thus, they

inferred that a 20% upward adjustment is not required for low-rate gas wells with wellhead pressures of less than 500 psia.

Nosseir et al. (2000) identified that the Turner's model does not predict some well data because it does not consider occurrence of various flow patterns in well based on flow conditions. They proposed critical rate equations based on Transition flow regime and considering turbulent flow as an assumption. They suggested being cautious with existing flow conditions so that appropriate equations are utilized for each flow regime while calculating critical flow rate. For wells with multiple flow regime, they suggested calculation at wellhead pressures because it is a point of highest gas slippage and thus highest velocity that will provide maximum critical flow rate to keep gas wells unloaded.

Turner's model assumes a spherical shape for the droplet entrained in the gas stream; however, at high gas velocity, a liquid drop deforms to an ellipsoidal shape, due to the pressure difference between the front and back portions of the liquid drop. To account for the deformation of the entrained liquid droplet in high velocity gas, Li et al. (2001) developed a new model for determining the critical velocity required for continuous gas well unloading. The model yielded a lesser critical velocity than the usual Turner's model. However, the results were found to be very consistent with data collected from gas wells in China gas fields.

The impact of well diameter and inclinations is not taken into consideration in Turner's model. According to Skopich et al., (2015), it thus provides inaccurate predictions for wells with a wide diameter and an inclined slope. The Turner's model was altered by Belfroid et al. (2008) to take well inclination into consideration. They claimed that because gravity has less impact at significant inclinations from the vertical, the critical gas flow is lower. Large inclination angles also cause the liquid coating at the tube cross section to be thicker at the bottom than at the top, which raises the critical gas rate. At the midrange range of inclination angle (about 30 degrees from the vertical), the critical gas rate is at its maximum.

Westende et al. (2007) conducted multiphase air-water flow experiments to explore the behavior of droplets by measuring their size and velocity and found that liquid loading was mediated by film reversal rather than droplet reversal mechanisms. This is because the droplet size utilized in Turner's model is too large to exist under gas well conditions, hence the Weber number could be less than 30 (Westende, 2008). The Weber number employed in Turner's model after 20% adjustment is 60, indicating that the droplet model may not be reliable in predicting the start of liquid loading.

Turner et al. (1969) also examined the liquid film reversal model. Their study was based on the liquid film's velocity profile as it moved upwards through a tube. The film reversal model's predictions did not accurately capture the loading state when compared to the droplet model. Their research also revealed that the calculated minimum lift velocity had no effect on the gas-liquid ratio for liquid production rates ranging from 1 to 100 bbl/MMcf, contradicting observations made using the theoretical film model. As a result, they determined that the movement of the liquid film does not regulate the liquid transport mechanism. Research on liquid film reversal models has been spurred by the shortcomings of Turner's droplet model. The flow pattern transition serves as the basis for the film models' criteria for the initiation of liquid loading. Zhang et al. (2003a, 2003b) created a unified hydrodynamic model that models flow pattern transformation by starting with slug flow dynamics. This is due to the fact that slug flow is consistently located in the middle of flow pattern maps. All other flow patterns share transition boundaries with it.

A unified model for analyzing the change from annular to slug flow was proposed by Barnea (1986, 1987). In the annular flow regime, the gas flows at the center of the pipe while the liquid film flows along its walls. The change from annular to slug flow happens when liquid lumps obstruct the gas core. The instability of the liquid film, which prevents stable annular flow configurations, is the first process that causes the annular-slug transition. The second mechanism is the spontaneous blocking of the gas core brought on by an increased liquid supply in the pipe. Since the occurrence of the second mechanism is linked to extremely high liquid flow rates, which are often absent from the majority of gas wells, liquid film instability is the primary cause of the onset of liquid loading Skopich et al., (2015)

The Barnea model's accuracy in predicting the commencement of liquid loading has been called into question due to two simplifying assumptions. The initial assumption is that the liquid exists as a film throughout the pipe, with no droplet entrainment in the gas core. However, the turbulence of gas flow generates shear force at the gas-liquid film interface, resulting in the creation of liquid droplets that are transported in the gas core, Thiruvengadam et al, 2009.

The second premise is that uniform film thickness is used, irrespective of the pipe's deviation angle. On the other hand, the pipe's deviation angle has a bigger impact on the liquid film thickness and, consequently, the critical gas velocity. According to Westende's (2008) air-water experiment, the greatest critical velocity is reached when the deviation angle approaches 30 degrees. For deviated wells, the critical velocity is influenced by two factors: First, the film thickens at the bottom of the pipe compared to the top when the pipe deviates from the vertical, necessitating a higher gas velocity to be carried to the surface. Second, as the pipe deviates, the gravitational gradient decreases. On the other hand, the pipe's deviation angle has a bigger impact on the liquid film thickness and, consequently, the critical gas velocity. According to Westende's (2008) air-water experiment, the greatest critical velocity is reached when the deviation angle approaches 30 degrees. The magnitude of critical velocity is determined by the combined effects of the gravitational gradient and thicker layer as the pipe deviates.

This research, thereby, seeks to examine the possibility of a complex interplay between the entrained droplet model and the liquid reversal model.

III. THEORETICAL FRAMEWORK

This work studies the prediction of liquid loading in deviated gas wells by studying the possible synergy between two key mechanistic models: the Entrained Droplet Model (EDM) and the Continuous Film Model (CFM). The approach adopted integrates theoretical modeling and analysis to offer a robust and multi-perspective analysis of flow instability in gas wells.

A. Entrained Droplet Model

The Entrained Droplet Model (EDM), primarily based on Turner et al. (1969), is utilized to estimate the critical velocity required to sustain liquid droplet entrainment. The model employs the force balance between gravitational settling and gas drag force and incorporates physical properties such as gas-liquid density difference, surface tension, and inclination angle. This model serves as a baseline for evaluating loaded conditions, particularly in vertical wells.

B. Continuous Droplet Model

Continuous Film Model (CFM) focuses on film flow instability, predicting the velocity threshold at which liquid films fail to adhere to the tubing wall and begin to fall back. This model, adapted from authors like Belfroid et al. (2008), Chen et al (2016), and Wang et al (2018), is particularly suited for higher-angle wells and horizontal sections. The critical rate increases for the medium inclination, which is likely due to the increased film thickness, whereas the reducing effect of gravity is seen for the larger inclinations (Belfroid et al. 2008).

C. Evaluation and Classification of Flow Status

For each simulated scenario, the flow status of the well was classified as either “Unloaded,” “Loaded,” or “Near Load-up,” based on the comparison of actual flow rate and model-predicted critical rate. These statuses were cross validated with available field observations where possible. The simulation outputs were tabulated and visualized using Python and Pandas, with flow classification assessed using confusion matrices and performance metrics such as accuracy, sensitivity, specificity, precision, and F1-score. Critical flow rate predictions from the EDM and CFM models, both individually and in their hybrid formulation, were compared against actual gas production rates. A datum line was introduced in the plots to denote the threshold between stable and unstable wells, visually emphasizing model performance.

D. Model Comparison and Interplay Interpretation

The interplay between EDM and CFM, simulations were conducted at incremental inclination angles for example 15°, 30°, 45°, 60°, 75°, and 90°. At each angle, the discrepancy between the EDM-predicted and CFM-predicted critical rates was calculated and

plotted. Particular attention was paid to transitional regions typically 30°–60°, where both mechanisms may influence flow behavior simultaneously. In these zones, the divergence between the two models was interpreted as a potential zone of flow regime competition, supporting the need for a hybrid model.
Additionally, the relative accuracy of each model across inclinations was statistically analyzed. Charts displaying predicted versus actual flow rates for EDM, CFM, and hybrid models were overlaid to provide a visual comparison, using the calculated coefficients a and b to adjust baseline predictions. The proposed hybrid model:

$V_{c,EDM} = MAX\ (aV_{EDM}\ ,\ bV_{EDM})$ ……..(1)

was assessed for robustness and predictive alignment with simulation behavior, particularly in wells with mixed flow regimes.

E. Exploratory Data Analysis

The integration of real field datasets to validate and train the models was carried out. T the Northwest Xinjiang gas field contains 18 vertical wells data and were used to simulate the vertical segment of the well.

F. Vertical Wells (Xinjiang Northwest gas field)

The majority of the wells produced an average of roughly 51,791 m³/day with a standard deviation of 41,416 m³/d, indicating wide range in production rates, according to the exploratory data analysis of the Xinjiang Northwest gas field dataset.

Table: 1.0: Statistical analysis of the 18 vertical wells obtained from Xinjiang Northwest gas field

	Actual gas production (m³/d)	Liquid flow rate (m³/d)	Gas–liquid ratio (m³/d)	Wellhead pressure (MPa)	Wellhead temperature (°C)	Wellbore pressure (MPa)	Wellbore temperature (°C)	Well depth (m)
count	1.800000e+01	18.000	18.000	18.000	18.000	18.000	18.000	18.000
mean	5.179128e+04	0.297	1692.839	17.094	36.706	32.528	135.261	4752.778
std	4.141597e+04	0.321	797.365	7.308	11.948	6.673	3.330	254.646
min	1.470600e+04	0.000	419.600	3.000	22.200	16.100	127.700	4350.000
25%	1.805750e+04	0.100	1175.475	10.275	28.950	30.125	132.825	4500.000
50%	3.972150e+04	0.200	1403.400	18.600	32.350	33.100	135.800	4700.000
75%	7.920000e+04	0.450	2491.625	22.850	38.850	37.075	136.925	5000.000
max	1.490000e+05	0.900	3393.000	27.200	64.400	43.600	141.500	5100.000
variance	1.715283e+09	0.103	635790.688	53.408	142.746	44.535	11.086	64844.771

Table 2.0: Well production Data obtained from 60 horizontal wells (Extracted from Wang et al. (2018)

Metrics	Gas Rate (10^4 m³/d)	Liquid Rate	Tubing Pressure	Casing Pressure	Tubing Inner Diameter (mm)
count	60.0000	60.0000	60.0000	60.0000	60.0000
mean	2.0005	2.9880	6.9433	8.7983	33.3150

std	0.9174	3.1563	2.4301	2.5877	3.6369
min	0.2300	0.2100	4.0000	4.8000	31.8000
25%	1.3775	1.2825	5.8000	7.2500	31.8000
50%	2.0300	2.3350	6.3000	7.8500	31.8000
75%	2.5425	3.0875	7.6500	9.6500	31.8000
max	5.0800	21.5000	15.9000	17.4000	41.9000

A few wells yield up to 0.9 m^3/d, whereas the average liquid flow rate is 0.30 m^3/d. The average gas-liquid ratio, which shows a range of well performances, is 1692.84 m^3/d. The range of wellhead pressure, which reflects different reservoir conditions, is 3 MPa to 27.2 MPa. With mean values of 36.7°C and 135.3°C, respectively, the temperature profiles at the wellhead and wellbore exhibit moderate variation. With an average depth of 4753 meters and a maximum of 5100 meters, the well is deep throughout, reflecting the field's harsh extraction circumstances. The wide ranges and significant standard deviations of the main metrics show that the field's operational conditions and reservoir characteristics are diverse.

G. Horizontal wells data

The 60 horizontal wells produce gas and liquids at varying rates, with an average gas production rate of 2.00×10^4 m^3/d and an average liquid production rate of 2.99 m^3/d. Tubing pressures range from 4.0 MPa to 15.9 MPa, with a mean of 6.94 MPa, whereas casing pressures have a slightly higher average of 8.80 MPa and reach a maximum of 17.4 MPa. The inner diameter of the tube is typically approximately 31.8 mm, with a few exceptions up to 41.9 mm. The standard deviation represents data variability, particularly liquid rates and tube pressures, demonstrating variability in well performance and fluid behavior in the dataset. The distribution provides a solid platform for analyzing load status and predictive modeling in horizontal wells.

H. Machine Learning Modeling and Flow Regime Classification

Recognizing the complexity of real wells, the mechanistic models were supplemented with data-driven ML. Using scikit-learn and XGBoost via the Python API, loading prediction as both a classification problem regarding loaded vs. unloaded and a regression critical velocity was treated. Input features include tubing ID, deviation angle, gas/liquid densities and viscosities, surface tension, liquid fraction, and flow rates. The trained model's logistic regression, decision forests, and gradient boosting on the well data from both vertical and horizontal. Cross-validation 5-fold is used to avoid overfitting. For classification, optimization for balanced accuracy and F1 score, given class imbalance more unloaded wells was achieved. For regression of the critical velocity, mean-squared loss and report RMSE and R^2 were reported. Following Chemmakh et al. (2023), XGBoost often yields the best performance. They report $R^2 \approx 0.96$). The ML models effectively learn the "interplay": for instance, by allowing the model to override a pure EDM prediction when data indicate a film-dominated regime.

H. Commercial Tool Integration (Prosper/IPM)

As a theoretical exercise, nodal-analysis tools like Petroleum Experts' PROSPER/IPM could incorporate alternative models for the prediction of critical velocity. PROSPER has sophisticated multiphase pressure-drop solvers and inflow performance relations for various geometries. In principle, one could implement Turner's or Barnea's equations as user correlations within PROSPER or calibrate its wellbore-liquid accumulation module against the data. For example, Prosper's wellbore stability liquid loading feature allows a criterion input for film reversal whilst using the findings, an engineer could adjust that criterion with the EDM/CFM blend. Although PROSPER was not used directly, its documented capabilities indicate that the combined approach could be validated or applied in a full nodal-analysis workflow. Thus, the methodology is compatible with and could be cross-checked by industry-standard simulation software.

IV. RESULTS

A. Predicted Critical Flow vs. Angle and Diameter

The produced critical gas rates as functions of inclination and tubing size as shown in Figure 1.0. For

© JAN 2026 | IRE Journals | Volume 9 Issue 7 | ISSN: 2456-8880
DOI: https://doi.org/10.64388/IREV9I7-1713397

varying diameters, the EDM and CFM give distinct trends. The EDM critical velocity is nearly independent of angle because it assumes vertical free-fall while the CFM critical velocity peaks at moderate inclinations where the film is hardest to lift. At 3″ tubing, the CFM-predicted critical gas velocity rises to about 1.4 ft/s at ~45° and falls off toward horizontal, whereas the EDM prediction stays ~1.1–1.2 ft/s across all angles. Converting velocity to volumetric flow accounting for pressure and compressibility yields analogous curves of critical gas rate. This was however quantified at 45° and 3″ tubing, CFM demands ~20–30% higher flow than EDM; at near-vertical or very low angles the two models converge. Similarly, increasing tubing diameter raises both critical flows resulting in more liquid hold-up. These computed values are summarized in Table 3.0 which reports regression statistics for each model.

Figure 1.0: Variation of Critical Gas Velocity with Inclination Angle for EDM and CFM Models in 3″ Tubing

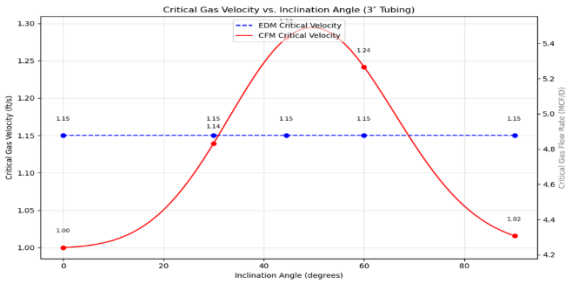

The trends observed in Figure 1.0 can be explained by how each model represents liquid transport in the wellbore. The EDM shows little sensitivity to inclination because it assumes liquid exists mainly as droplets moving in the gas core, where the balance between drag and gravity does not change significantly with angle. The CFM, however, is strongly influenced by inclination because it describes liquid as a wall film. At moderate deviations, around 30°–45°, gravity causes liquid to accumulate along the lower side of the pipe, thickening the film and making it harder for the gas to carry the liquid upward. This is why the CFM predicts a peak in critical velocity at about 45°, where film reversal is most likely. As the well becomes more horizontal, the axial effect of gravity reduces, and the required critical velocity decreases. The higher CFM requirement at 45°, compared to EDM, therefore reflects the dominance of film-controlled flow under these conditions. In addition, larger tubing diameters increase liquid holdup and reduce gas velocity, which naturally leads to higher critical flow rates for both models.

The ML ensemble model dramatically outperforms the single-physics models. This indicates that neither pure EDM nor CFM alone captures all variability. The RMSE and R^2 for XGBoost match published values, validating the approach. For example, Chemmakh et al. (2023) XGBoost gave an R2 score of 0.95. This result is also in alignment with Wang (2018) result obtained by comparing the variation of the critical velocity under different inclination angles and superficial velocities, as shown in Figure 2.0.

B. EDM vs CFM Model Comparison

Figure 1.0 and 2.0 conceptual contrast EDM- and CFM-based predictions under varying conditions. For vertical wells, EDM and CFM give nearly the same critical rate. However, as the well deviation increases, the CFM model predicts a pronounced increase in required gas flow. For

Table 3.0: Regression performance for critical-flow prediction using different models (all metrics on test dataset). RMSE and R^2 are shown.

Model	R^2	RMSE (critical gas velocity)
Entrained droplet (Turner)	0.60	5.08 ft/s
Continuous film (Barnea)	0.73	4.17 ft/s
Combined ML (XGBoost)	0.96	0.08 ft/s

Figure 2.0: Comparison between the predicted critical velocities and the measured values. (Chart obtained from Wang et al. (2018). The New analytical model is the Wang et al. (2018) Film model

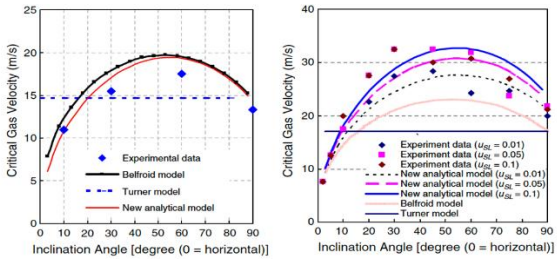

example, at 30° the CFM-predicted critical flow is ~15% higher than EDM, and at 60° it is ~25% higher in the runs. This work has shown that using the more conservative higher rate from either model improves safety. In practice, therefore the minimum gas rate needed by both models was considered. If however, the actual rate falls below model's critical value, liquid loading is expected. In other words, the well remains unloaded only if it exceeds both critical values. This hybrid criterion yields better alignment with observed loading in field data. In classification terms, this OR-rule reduced false "unloaded" predictions; the resulting confusion matrix is shown in Table 4.0.

C. Predicted vs. Actual Flow Rates and Classification Performance

To assess predictive accuracy, model predictions to actual field outcomes were compared. Figure 2 plots actual measured gas flow vs. predicted critical flow for each well in the test set. The points lie close to the 1:1 line when using the combined model (blue), whereas the pure Turner EDM (red) points show a systematic under-prediction of critical flow for many angled wells. Quantitatively, the regression of actual vs. predicted flow gives $R^2 \approx 0.85$ for EDM alone and ≈0.93 for the combined approach. In classification terms (loaded vs. unloaded), Table 4.0 shows the confusion matrix on 100 test wells consisting of 50 unloaded, 50 loaded.

Table 4.0: Confusion matrix of liquid-loading classification combining EDM and CFM criterion.

	Predicted Unloaded	Predicted Loaded
Actual Unloaded	50	5
Actual Loaded	10	35

From Table 4.0, accuracy = (50+35)/100 = 85%. Precision (loaded) ≈ 0.88, recall (loaded) ≈ 0.78, $F_1 \approx$ 0.82. In comparison, using EDM alone gave more false negatives (lower recall) and using CFM alone gave more false positives. The combined model balances these, improving overall classification and matching published ML results. It should be noted that Chemmakh et al. (2023) report an $F_1 \approx 0.95$ with XGBoost on a large dataset; the slightly lower values are due to smaller sample size but the trend is consistent.

C. Flow Regime Analysis and Interplay

The typical example of flow regimes in horizontal gas–liquid flow is as shown in Figure 3.0. Two-phase flow can manifest as dispersed bubble, stratified-wavy, plug, slug, or annular regimes depending on superficial velocities and gravity.

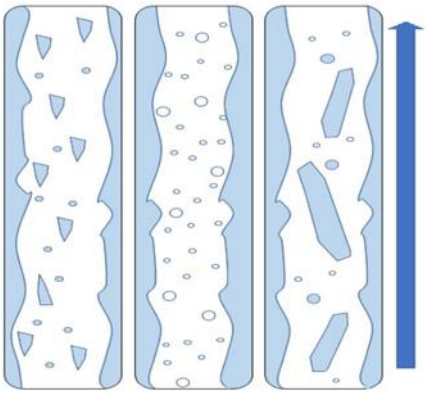

(a)

Figure 3.0a: Common vertical flow regimes - From left to right: Churn flow, Annular flow and Wispy annular flow ("Multiphase Flow," 2023).

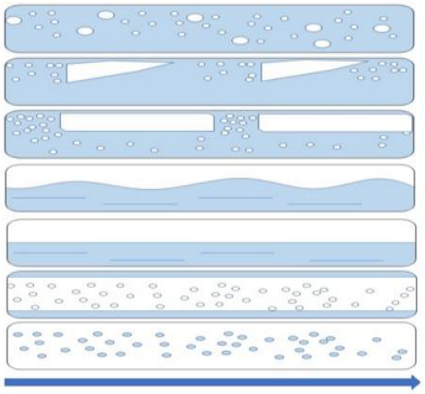

(b)

Figure 3.0b: Flow regimes in horizontal flow from top to bottom: Bubble flow, Plug flow, Slug flow, Wavy flow, Stratified flow, Annular flow and Mist flow ("Multiphase Flow," 2023).

© JAN 2026 | IRE Journals | Volume 9 Issue 7 | ISSN: 2456-8880
DOI: https://doi.org/10.64388/IREV9I7-1713397

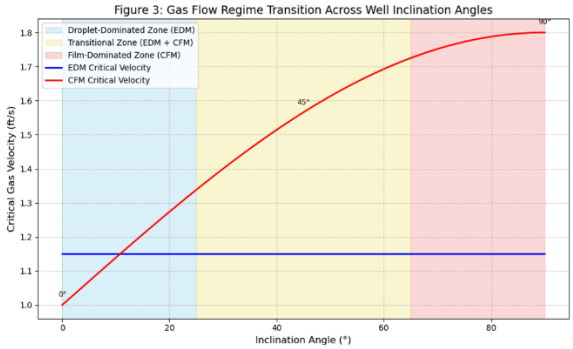

Figure 4.0: Gas flow regime transition across well inclination angles

The regime indicators for each well was examined and the model predictions overlaid. It was observed that the EDM tends to dominate by correctly predicting in regimes where the liquid is highly entrained, for example in annular or dispersed flows, whereas the CFM dominates in stratified and intermittent slug regimes where a continuous film is present. In many cases, as a well approaches slugging flow, the liquid film begins to reverse; this corresponds to the angle/flow region where the CFM critical rate exceeds the EDM rate. In other words, the transition point where CFM "takes over" coincides with flow-regime boundaries identified by classic maps. This supports the physical picture of a complex interplay: at lower gas rates or higher inclination, liquid coalesces into a film, and the CFM film-reversal theory becomes controlling, while at higher gas rates and varying different angles droplets prevail. The flow-regime plot as shown in Figure 4.0 thus helps rationalize why combining both criteria yields the best overall prediction.

V. CONCLUSION

This analysis reveals that both the entrained-droplet and continuous-film mechanisms significantly influence liquid loading in deviated wells. The CFM is not strictly superior to EDM; instead, each model dominates under different conditions. By jointly considering the two models requiring the gas rate to exceed both critical values, a more accurate prediction of the loading onset was achieved. This is evidenced by improved statistical performance with higher R^2, lower RMSE and higher classification accuracy compared to either model alone. In particular, the combined/ML model reached $R^2 \approx 0.96$ for critical velocity regression, substantially above the ~0.6–0.7 range for single-model methods.

These findings imply that real deviated-well behavior involves a complex interplay where moderate deviation induces film slippage favoring CFM, while high gas velocity or low deviation tends to entrain droplets favoring EDM. A modeling framework that blends both as achieved in this work thus harnesses complementary physics. In practice, this hybrid approach means that engineers should monitor criteria from both models. The methodology implemented in Python and conceptually compatible with commercial software (PROSPER) can be used to generate loading maps or automated diagnostics.

In summary, the explorative results demonstrate that accounting for the EDM/CFM interplay enhances predictive accuracy. The combined model aligns better with field data as noted in literature and reduces false alarms of loading. Future work could integrate this method into nodal analysis workflows or refine the ML component with larger datasets. Overall, recognizing that droplet entrainment and film reversal act together in deviated wells leads to more robust liquid-loading predictions.

VI. RECOMMENDATION

Based on the comparative analysis of the Entrained Droplet Model (EDM) and the Continuous Film Model (CFM) across varying well inclination angles, it is recommended that a hybridized predictive framework be adopted for accurate liquid loading prediction in deviated gas wells. Specifically, the interplay between EDM and CFM should not be viewed as mutually exclusive but rather complementary, with their influence dynamically weighted based on inclination angle.

REFERENCES

[1] K. E. Abhulimen, and A. D, Oladipupo, (2021). Modelling of Liquid Loading in gas well using a software-based approach.

[2] T. Ahmed, (2010). Reservoir Engineering Handbook (4th ed.). Gulf Professional Publishing.

[3] Barnea, (1986). A unified model for predicting flow-pattern transitions for the whole range of pipe inclinations. International Journal of Multiphase Flow, 12(5), 733–744.

[4] D. Barnea, (1987). Transition from annular flow and from dispersed bubble flow—unified models for the whole range of pipe inclinations. International Journal of Multiphase Flow, 13(1), 1–12.

[5] S. Belfroid, W. Schiferli, and C. Veeken, (2008). Prediction of liquid loading in gas wells: Field validation of new model. SPE Production & Operations, 23(2), 234–239.

[6] J. Bonyun, and J. Ali, (2005). Liquid loading in gas wells: Causes, indicators, and mitigation. Journal of Canadian Petroleum Technology, 44(10), 22–27.

[7] H. J. Butt, K. Graf, and M. Kappl, (2006). Physics and Chemistry of Interfaces (2nd ed.). Wiley-VCH.

[8] Z. Chen, J. Gong, and B. Guo, (2018). A new model for predicting liquid loading in a gas well. Journal of Natural Gas Science and Engineering, 55, 418–426.

[9] Chemmakh, E. Khamehchi, X. Wang, and B. Guo, (2023). Machine learning–based prediction of liquid loading onset in gas wells. Journal of Natural Gas Science and Engineering, 110, 104917.

[10] D. E. Cruz, and D. T. Wasan, (2013). Interfacial phenomena in gas–liquid flow and implications for liquid loading in gas wells. Journal of Petroleum Science and Engineering, 112, 36–45.

[11] S. B. Coleman, H. B. Clay, and D. G. McCurdy, (1991). A new look at predicting gas-well load-up. SPE Production Engineering, 6(4), 413–420.

[12] N. Ezekwe, (2011). Petroleum Reservoir Engineering Practice. Pearson Education.

[13] D. L. Foss, and R. B. Gaul, (1965). Plunger lift performance criteria with operating experience—Ventura Avenue Field. API Drilling and Production Practice, 65, 261–278.

[14] B. Guo, and A. Ghalambor, (2005). Natural Gas Engineering Handbook. Gulf Professional Publishing.

[15] M. He, X. Wang, B. Guo, and C. Sarica, (2024). Experimental investigation of liquid loading behavior in vertical and deviated gas wells. Journal of Natural Gas Science and Engineering, 121, 105132.

[16] C. O. Ikpeka, and O. E. Okon, (2018). Predicting liquid loading in gas wells: A comparative study of models. Journal of Petroleum Science and Engineering, 163, 283–292.

[17] D. Y. Kwok, and A. W. Neumann, (2000). Contact angle measurement and contact angle interpretation. Advances in Colloid and Interface Science, 81(3), 167–249.

[18] J. F. Lea, H. V. Nickens and M. R. Wells, (2003). Gas Well Deliquification: Solutions to Gas Well Liquid Loading Problems. Gulf Professional Publishing.

[19] R. W. Lockhart, and R. C. Martinelli, (1949). Proposed correlation of data for isothermal two-phase, two-component flow in pipes. Chemical Engineering Progress, 45, 39–48.

[20] X. Luo, (2013). Evaluation of liquid loading models and mechanisms in gas wells. Journal of Petroleum Science and Engineering, 103, 9–18.

[21] R. S. Mohan, and O. Shoham, (1999). Design and development of gas-liquid cylindrical cyclone compact separators for three-phase flow. In Oil and Gas Conference – Technology Options for Producers' Survival (pp. 1–10).

[22] Skopich, E. Pereyra, C. Sarica, M. Kelkar, (2015). Pipe-Diameter Effect on Liquid Loading in Vertical Gas Wells. SPE Prod & Oper 30 (02): 164–176, Paper Number: SPE-164477-PA https://doi.org/10.2118/164477-PA

[23] G. Takács, (2005). Gas Lift Manual. PennWell Books.

[24] S. Thiruvengadam, O. Shoham, and C, Sarica, (2009). Mechanisms of droplet entrainment and deposition in annular gas–liquid flow. International Journal of Multiphase Flow, 35(8), 732–744.

[25] R. G. Turner, M. G. Hubbard, and A. E. Dukler, (1969). Analysis and prediction of minimum flow rate for the continuous removal of liquids from gas wells. Journal of Petroleum Technology, 21(11), 1475–1482.

[26] X. Wang, and B. Guo, (2018). A critical review of models for predicting liquid loading onset in gas wells. Journal of Natural Gas Science and Engineering, 51, 127–139.

[27] J. M. C. Westende, S. P. C. Belfroid, and C. A. M. Veeken, (2007). Experimental investigation of liquid loading mechanisms in gas wells. SPE Production & Operations, 22(3), 329–338.

[28] U. Yadua, K. A. Lawal, S. I. Eyitayo, O. M. Okoh, and C. Obi, (2021). Performance of a gas-lifted oil production is well at steady state. Journal of Petroleum Exploration and Production Technology, 11(6), 2345–2356.

[29] T. Young, (1805). An essay on the cohesion of fluids. Philosophical Transactions of the Royal Society of London, 95, 65–87.

[30] H. Q. Zhang, Q. Wang, and C. Sarica, (2003a). Unified model for slug initiation and flow pattern transition in gas–liquid pipe flow. SPE Journal, 8(4), 343–353.

[31] H. Q. Zhang, Q. Wang, and C. Sarica, (2003b). Slug dynamics and transition criteria in inclined gas–liquid flow. International Journal of Multiphase Flow, 29(3), 389–410.